Information cascades on degree-correlated random networks

Joshua L. Payne,[1,2] Peter Sheridan Dodds,[2,3] and Margaret J. Eppstein[1,2]
[1]*Department of Computer Science, The University of Vermont, Burlington, Vermont 05405, USA*
[2]*Complex Systems Center & The Vermont Advanced Computing Center, The University of Vermont, Burlington, Vermont 05405, USA*
[3]*Department of Mathematics and Statistics, The University of Vermont, Burlington, Vermont 05405, USA*
(Received 13 March 2009; revised manuscript received 5 June 2009; published 25 August 2009)

We investigate by numerical simulation a threshold model of social contagion on degree-correlated random networks. We show that the class of networks for which global information cascades occur generally expands as degree-degree correlations become increasingly positive. However, under certain conditions, large-scale information cascades can paradoxically occur when degree-degree correlations are sufficiently positive or negative, but not when correlations are relatively small. We also show that the relationship between the degree of the initially infected vertex and its ability to trigger large cascades is strongly affected by degree-degree correlations.

DOI: 10.1103/PhysRevE.80.026125 PACS number(s): 89.75.Hc, 89.65.−s, 05.45.−a, 87.23.Ge

I. INTRODUCTION

Many real-world networks have been shown to exhibit correlations between degrees of adjacent vertices. For example, social interaction networks are typically found to be *assortative* (i.e., degrees of adjacent vertices are positively correlated), while technological and biological networks are commonly *disassortative* (i.e., degrees of adjacent vertices are negatively correlated) [1,2]. Degree-degree correlations have been shown to have a significant impact on various network-based dynamical processes [1–7].

Here, we focus on the influence of degree-degree correlations on a threshold model of binary decisions, originally developed by Watts for uncorrelated generalized random networks [8]. In such threshold models, a vertex will change to a new state if a specified fraction of its neighboring vertices are in that state. The network is initialized by "seeding" a small number or fraction of vertices with a novel piece of information; when this information spreads throughout a significant portion of the network, it is referred to as an information cascade, akin to processes in real-world systems, such as propagating failures in power grids [9,10] or the adoption of new ideas and fads in social networks [11]. The size and frequency of such information cascades have been shown to be heavily influenced by various network properties [8,12–15], but the impact of degree-degree correlations is not yet completely understood.

A key aspect of this threshold model is that a single vertex may trigger a global cascade. In the context of technological networks, such as power grids, these "triggers" represent the system's Achilles' heel, whereas in social systems, they—at least theoretically—represent the prime targets for marketing strategists to effectively advertise their product [13,16]. Using this model, we perform extensive numerical simulations starting from a single initial seed on large ($N=10^4$) degree-correlated random networks and investigate the frequency and size of large-scale information cascades, as well as the underlying structure of a network's triggering component. Elsewhere, we develop analytic results concerning the frequency of global cascades on degree-correlated random networks [17], complementing the recent results of Gleeson [18], who provided analytic results for cascade sizes. However, we note that these analytic solutions are not solvable in an exact fashion, except for the case of highly specialized networks. Investigating the size and frequency of information cascades on generalized random networks with degree-degree correlations thus requires either numerical solutions to these analytic formulas or direct simulation. Here, we generally take the latter approach, as it is more transparent and less susceptible to numerical error, although we do make some comparisons to numerical solutions of analytic results.

II. MODEL

Vertices can be in one of two states, *active* (infected) or *inactive* (susceptible), and once a vertex activates, it cannot deactivate [8]. Every vertex is given an identical threshold-based response function, where the probability (Π) that a vertex of degree k changes its state from inactive to active is a function of the fraction of its k neighbors that are active. Specifically, if x denotes the number of active neighbors of a vertex of degree k and ϕ denotes the threshold of its response function, then

$$\Pi(x,k) = \begin{cases} 1 & \text{if } \dfrac{x}{k} \geq \phi \\ 0 & \text{otherwise.} \end{cases} \tag{1}$$

Vertices are updated synchronously, though for the case of monotonically increasing response functions, as considered herein, asynchronous updating yields equivalent results.

Vertices that activate in the presence of a single active neighbor are referred to as *vulnerable*, and all other vertices are referred to as *stable* [8]. Large-scale information cascades triggered by a single vertex can only occur in infinite random networks if there exists a sufficiently large connected component of vulnerable vertices [8]. This is referred to as the *vulnerable component*, its fractional size is denoted by S_v (all sizes are given as a proportion of the number of vertices N), and the set of vertices it contains is denoted by Ω_v. The frequency of information cascades is almost completely dictated by S_v since any initial placement in Ω_v will lead to a

cascade of size at least S_v. However, stable vertices that are directly adjacent to the vulnerable component can also trigger large-scale cascades since an initial seed placed in one of these vertices will ignite the vulnerable component. We will refer to these vertices as *peripheral* and denote the set of peripheral vertices as Ω_p, with size S_p. The union of the vulnerable and peripheral components $\Omega_e=\Omega_v\cup\Omega_p$ makes up what is referred to as the *extended vulnerable component* [8], the size of which we denote as S_e. In infinite random networks, S_e is exactly the number of vertices that can trigger a large-scale information cascade, so this quantity will be equivalent to the frequency with which large-scale cascades occur if the initial seed is randomly chosen. Vertices outside of Ω_e are referred to as *external*, the set of which is denoted by Ω_x.

We will define a *global information cascade* as any cascade that infects 1% or more of the entire network. This arbitrary distinction [8] is reasonable because the distribution of cascade sizes is generally bimodal with sizes either well above or well below 1% (except near the onset of the percolating vulnerable component, where the cascade size distribution obeys a power law [8]). Thus, the terms *average global cascade size* (S_{gc}) and *global cascade frequency* (F_{gc}) will refer to global cascades only, omitting the lower mode of the distribution, while *average cascade size* (S_{avg}) will be used to mean the average of all information cascades, combining both modes of the cascade size distribution.

III. METHODS

We consider undirected random networks of N vertices, with average degree z and a Poisson degree distribution $p_k=z^k e^{-z}/k!$. Random networks were generated by randomly placing $M=Nz/2$ edges between pairs of vertices selected with uniform probability. Duplicate edges were prohibited, resulting in an exact average degree z.

Following Newman [1], we use e_{jk} to denote the probability that a randomly chosen edge connects vertices with degree $j+1$ and $k+1$. The quantity $q_k=\Sigma_j e_{jk}$ is then the probability that a randomly chosen edge followed in a random direction leads to a vertex of degree $k+1$. Degree-degree correlations are quantified by their assortativity r, which is formally defined [1] as

$$r=\frac{1}{\sigma_q^2}\sum_j\sum_k jk(e_{jk}-q_jq_k), \tag{2}$$

where $\sigma_q^2=\Sigma_k k^2q_k-[\Sigma_k kq_k]^2$ is the variance of the distribution q_k. A network is said to be disassortative if $r<0$, uncorrelated if $r=0$, and assortative if $r>0$.

We generate networks with a given assortativity, within some error tolerance, using the following iterative shuffling routine. At each step, we first measure the assortativity of the network using Eq. (2). Two edges $\langle a,b\rangle$ and $\langle x,y\rangle$ are then chosen at random with uniform probability such that a,b,x,y are all distinct. If the observed assortativity is less than the desired assortativity then we swap the edges such that the two vertices with the larger degree are connected to one another and the two vertices with the smaller degree are connected together. To instead incrementally decrease assortativity, we connect the two vertices with the largest and smallest degree, and the two vertices of intermediate degree. (If either of the new edges were already present then we leave the network unchanged.) Shuffling continues until the observed assortativity is within 0.01 of the desired assortativity. This method exactly preserves the underlying degree distribution p_k since the degree of each vertex remains unchanged after a swapping event.

We have recently shown [17] that the condition for the onset of global spreading, triggered by a single initial seed, is

$$|\mathbf{A}|=0 \quad \text{where} \quad [\mathbf{A}]_{j+1,k+1}=\delta_{jk}q_k-kb_{k+1}e_{jk}, \tag{3}$$

and b_k is the probability that a degree k vertex is vulnerable [19]. Note that round-off errors in the numerical solution of Eq. (3) can lead to multiple locations in which this equation is satisfied; in the results shown herein, we used the extremal values of z where the determinant of $\mathbf{A}$ was numerically equal to zero.

The vulnerable (Ω_v), peripheral (Ω_p), extended vulnerable (Ω_e), and external (Ω_x) components were determined through direct measurement of the realized networks (as in [8]). The vulnerable component was found by removing all stable vertices from the network and then using a breadth-first-search algorithm to determine the largest connected component of vulnerable vertices. The peripheral component was then calculated as the set of all stable vertices connected to the vulnerable component in the original network, and the extended vulnerable component was calculated as the union of the vulnerable and peripheral components. The external component was calculated as the difference between the set of vertices in the original network and those in the extended vulnerable component.

IV. SIMULATION DETAILS

Preliminary experimentation at $r\in\{-0.5,0.0,0.5\}$ and $1000\leq N\leq 30\,000$ showed that results became asymptotically stable for networks of size $N>3200$, above which the size of average cascades (S), frequency of global cascades (F_{gc}), and size of global cascades (S_{gc}) did not vary significantly ($p>0.01$, unpaired t test for data with unequal variance, for all comparisons where global cascades occurred). Thus, in all simulations the number of vertices was held constant at $N=10^4$, consistent with [8].

We considered thresholds ϕ in the range [0.1, 0.35] in increments of 0.01. Unless otherwise specified, the average degree z was varied from 1.0 to 20.0 in increments of 0.2. Assortativities ranged from $r=-0.95$ to $r=0.95$, depending on z since the shuffling method presented in Sec. III suffers from some constraints. In particular, it is considerably more difficult to obtain extremely negative assortativities than it is to obtain extremely positive assortativities, and this effect is especially pronounced for low z (see [17] for details). In Table I, we present the lower and upper bounds of the assortativities of the networks generated for this study, as a function of z.

For each combination of z and r, ten network instances were generated. For each combination of network instance

TABLE I. Ranges of assortativity considered in this study, as a function of average degree z.

Average degree (z)	Range of assortativity (r)
$z<1.0$	$-0.50\leq r\leq+0.50$
$1.0\leq z<2.0$	$-0.70\leq r\leq+0.95$
$2.0\leq z<3.0$	$-0.85\leq r\leq+0.95$
$3.0\leq z<5.0$	$-0.90\leq r\leq+0.95$
$z\geq 5.0$	$-0.95\leq r\leq+0.95$

and threshold ϕ, the initial seed was placed in each vertex, meaning an independent simulation was performed for each of the $N=10^4$ initial placements, resulting in almost 10^{13} simulations.

V. RESULTS

We first investigate the influence of degree-degree correlations on the "cascade window" [8], which delineates the region in which global cascades can occur, as a function of the vertex threshold ϕ and average degree z. In order to concretely ascertain the lower boundary of average degree z for which global cascades occur, we carried out additional simulations on random networks with $0.2\leq z\leq 1.0$ (in increments of 0.05). In Fig. 1, we depict the frequency of global cascades as a function of vertex threshold ϕ and average degree z in disassortative [Fig. 1(a)], uncorrelated [Fig. 1(b)], and assortative [Fig. 1(c)] random networks. Frequencies were recorded as the proportion of all simulations that resulted in a global cascade, across all initial placements on each of the ten network instances, for each combination of ϕ and z. The results of our simulations (Fig. 1, shaded contours) are in excellent agreement with Eq. (3) (Fig. 1, asterisks), although this analytic solution occasionally under predicts the upper z boundary of the cascade window.

As shown in Fig. 1, the cascade window is influenced by degree-degree correlations. In general, increasing assortativity r expands the parameter range in which global cascades are observed (compare the shaded regions in Fig. 1, as the panels are read from left to right). Specifically, for $\phi\leq 0.25$, increasing r consistently decreases the minimum, and increases the maximum, average degree z for which global cascades occur (compare the heights of the shaded regions in Fig. 1, as the panels are read from left to right). In uncorrelated networks, global cascades were never observed with $\phi>0.25$ [Fig. 1(b)]. However, at low average degree z, global cascades were observed for thresholds ranging from $0.25<\phi\leq 0.33$, for both disassortative networks [Fig. 1(a)] and assortative networks [Fig. 1(c)].

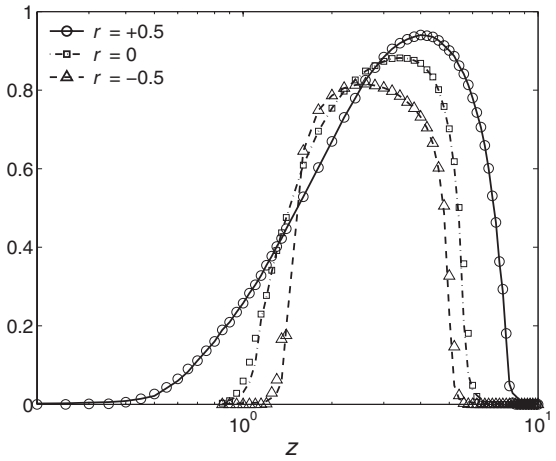

FIG. 2. Observed statistics of global cascades as a function of average degree z for $\phi=0.18$, on assortative ($r=+0.5$), uncorrelated ($r=0$), and disassortative ($r=-0.5$) random networks. Each data point is the frequency of global cascades observed on ten network instances. The lines correspond to the direct measurements of the extended vulnerable components (S_e). The x axis is scaled logarithmically.

In Fig. 2, we present the percolation phase transition in more detail, depicting both the observed frequencies of global cascades and the corresponding sizes of the extended vulnerable component (S_e), as a function of z. To be consistent with previous work [8,13], these cascade simulations pertain to a threshold of $\phi=0.18$, an arbitrary choice, for which vertices of degree $k\leq 5$ are vulnerable (corresponding to the vertical dashed lines in Fig. 1). For each value of r at $\phi=0.18$, we find excellent agreement between S_e (Fig. 2, lines) and global cascade frequency (Fig. 2, symbols), as

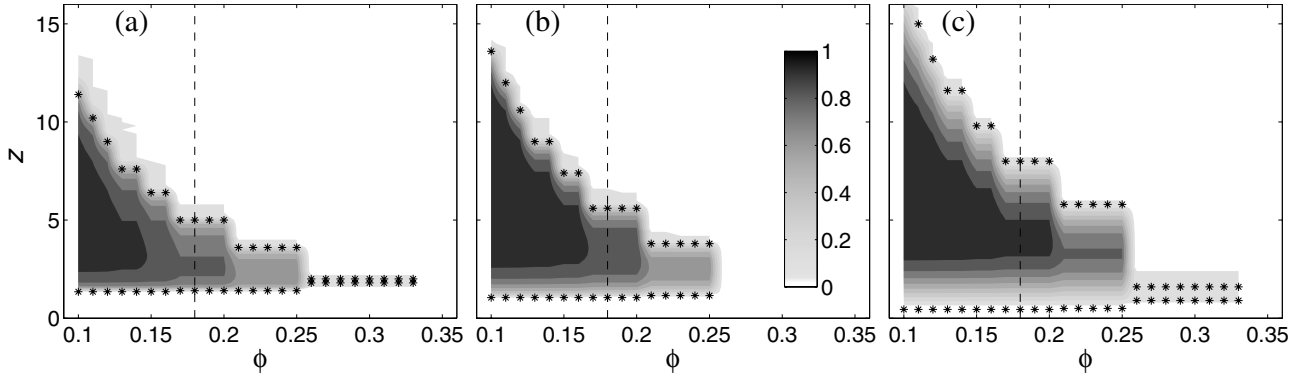

FIG. 1. Observed frequency of global cascades, as a function of threshold ϕ and average degree z, for (a) disassortative ($r=-0.5$), (b) uncorrelated ($r=0$), and (c) assortative ($r=+0.5$) random networks. The color bar corresponds to all panels. The asterisks denote the numerical solutions to Eq. (3). The dashed vertical lines at $\phi=0.18$ correspond to the three curves in Fig. 2.

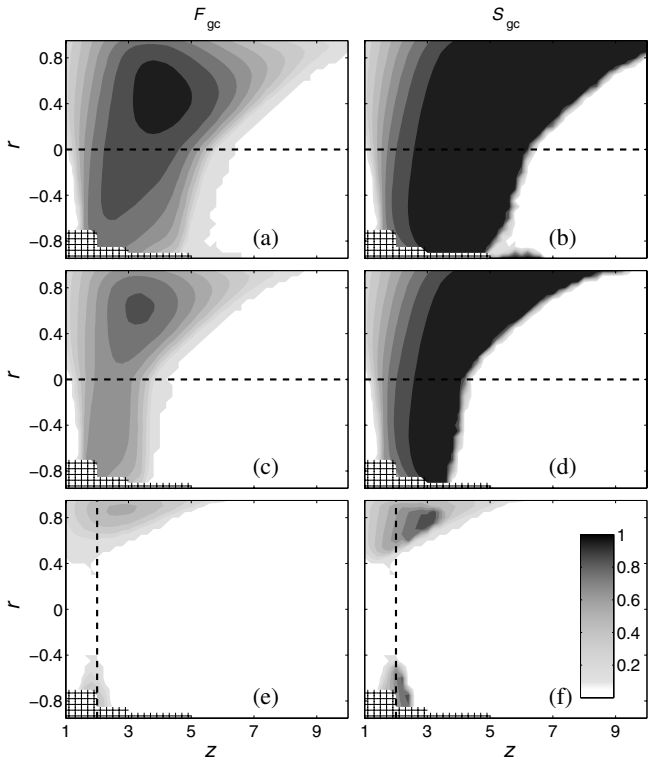

FIG. 3. Frequency (F_{gc}, left column) and size (S_{gc}, right column) of global cascades, as a function of average degree z and assortativity r, for three threshold values: $\phi=0.2$ (top row), $\phi=0.25$ (middle row), and $\phi=0.33$ (bottom row). The color bar corresponds to all panels. The dashed horizontal lines in panels (a)–(d) are at $r=0$, and the dashed vertical lines in panels (e) and (f) correspond to the data presented in Fig. 4. We were unable to obtain data in the hatched region (see Table I).

expected. Increasing r decreases the minimum z for which global cascades are observed and increases the maximum observed frequency of global cascades (compare the peaks of the three curves in Fig. 2). The range of z for which global cascades occur also increases with increasing r, as seen previously in Fig. 1. Further, increasing r alters the skew of the functional relationship between global cascade frequency and z (compare the shape of the curve as assortativity increases from $r=-0.5$ to $r=0$ to $r=+0.5$ in Fig. 2).

In Fig. 3, we depict the effects of average degree z and assortativity r on global cascade frequency (F_{gc}, Fig. 3, left column) and global cascade size (S_{gc}, Fig. 3, right column), for three vertex thresholds, $\phi=0.20$ (top row), $\phi=0.25$ (middle row), and $\phi=0.33$ (bottom row). For $\phi \leq 0.25$ and $r<0$, the maximum z for which any global cascades occur is relatively insensitive to changes in r [note how the right-most z boundary of the shaded contours below the horizontal dashed lines in Figs. 3(a) and 3(c) are nearly independent of r]. However, for $r>0$, the maximum average degree z for which global cascades occur increases dramatically as r becomes increasingly positive [Figs. 3(a) and 3(c), data above horizontal dashed line, where the right-most z boundary of the shaded contours increase rapidly with r]. Although the frequencies of global cascades near this upper-z boundary are low, when global cascades do occur they consistently spread

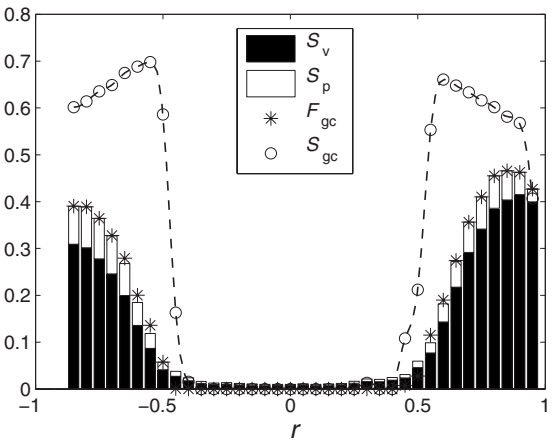

FIG. 4. Frequency (asterisks) and size (circles) of global cascades, as a function of assortativity r, for $z=2.0$ and $\phi=0.33$. The bars correspond to the sizes of the vulnerable (S_v, black) and peripheral (S_p, white) subcomponents of S_e. The dashed line is provided as a guide for the eyes.

throughout the entire network [as indicated by the black contours in Figs. 3(b) and 3(d); e.g., for $z=9$ and $r=+0.8$, compare the low frequency in Fig. 3(a) to the large cascade size in Fig. 3(b)].

A counterintuitive finding is that at high thresholds ($\phi > 0.25$, Fig. 3, bottom row) and low z, the frequency and size of global cascades becomes a bimodal function of r [Figs. 3(e) and 3(f)]. In addition, the sizes of global cascades near the upper-z boundary are significantly reduced relative to lower thresholds [as shown by the lower grayscale contours in Fig. 3(f) as compared to Figs. 3(b) and 3(d)]. Further details of the bimodal response to r at $z=2$ and $\phi=0.33$ [vertical lines in Figs. 3(e) and 3(f)] are depicted in Fig. 4, where we also show the sizes of the vulnerable (S_v) and peripheral (S_p) components. Note the sharp transition in global cascade size at $|r| \sim 0.5$ and how the global cascade size decreases as the frequency of global cascades increases for $|r| \to 1$.

Although the two modes shown in Fig. 4 look similar, they are caused by distinctly different underlying topological properties. In disassortative networks [e.g., Figs. 5(a)–5(c)], the vulnerable component comprises edges between vertices of alternating high and low degrees. For example, the vulnerable component shown in Fig. 5(b) for $z=2$ and $\phi=0.33$ comprises alternating vertices of degree $k=2$ and $k=3$, with only a few degree $k=1$ vertices attached. This results from the inherent negative degree correlation, where $k=1$ vertices frequently connect to stable vertices [$k>3$, Fig. 5(a)], excluding them from the vulnerable component. In contrast, for assortative networks [e.g., Figs. 5(g)–5(i)], vertices of similar degree are frequently connected in the vulnerable component. This is shown for networks with $z=2$ and $\phi=0.33$ in Fig. 5(h), where there are clusters of vertices of $k=3$ and chains of vertices with $k=2$, most of which are terminated by $k=1$ vertices. The probability of stable ($k>3$) vertices connecting to the core of $k=2$ and $k=3$ vertices is higher in disassortative networks [Fig. 5(a)] than in assortative networks [Fig. 5(g)]. Consequently, the peripheral component of $k>3$ vertices is larger in the disassortative networks [Fig.

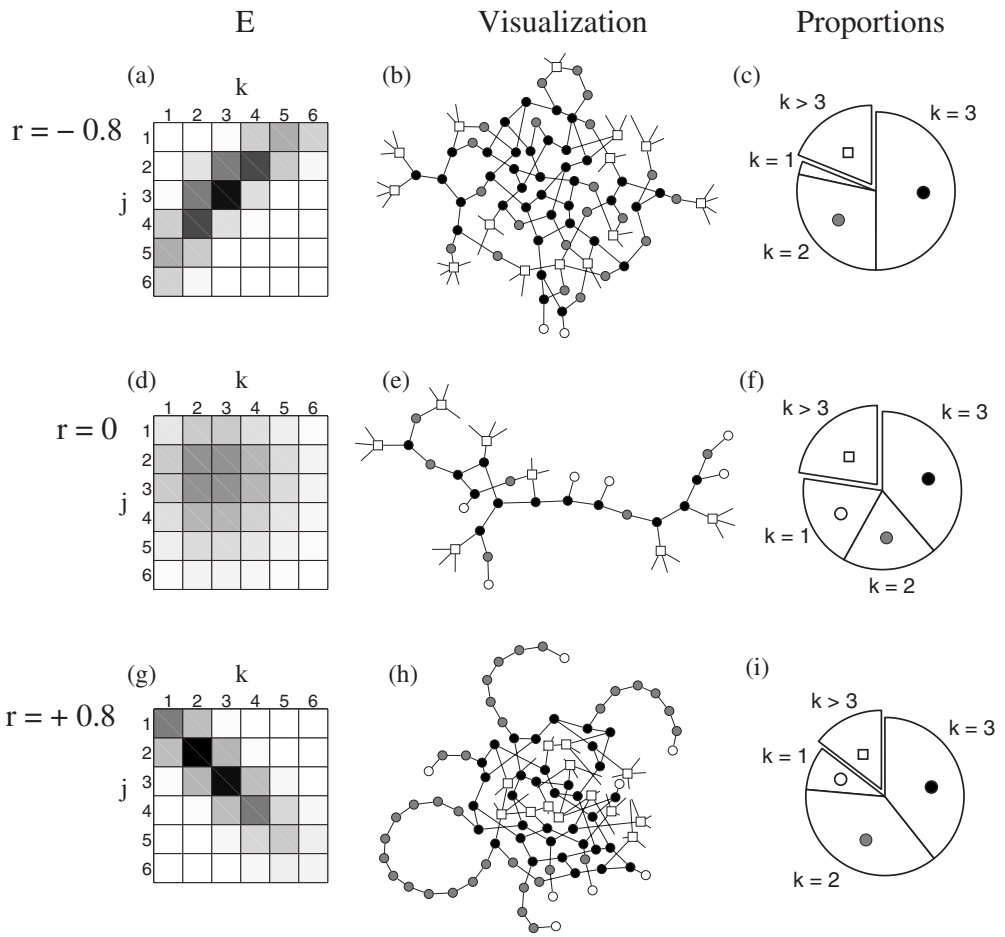

FIG. 5. Visualizations of random network properties with $z=2$ and disassortative ($r=-0.8$, top row), uncorrelated ($r=0$, middle row), and assortative ($r=+0.8$, bottom row) degree-degree correlations. In (a), (d), and (g), we visualize averages of the E matrices for all ten network instances ($N=10\,000$) used at each parameter combination. Shading (ranging from white to black) of matrix entries in E correspond to the probabilities (ranging from 0 to 0.17) with which a randomly chosen edge connects vertices of degree j and k; entries corresponding to vertices with $k>6$ occur with very low frequency and so are not shown. In (b), (e), and (h), we depict the extended vulnerable component (S_e) for $\phi=0.33$ for individual random networks with $N=200$ (for visual clarity). Peripheral vertices ($k>3$) are denoted as white squares; vertices in the vulnerable component are denoted as circles and are colored according to degree: white ($k=1$), gray ($k=2$), and black ($k=3$). The corresponding pie charts in (c), (f), and (i) denote the proportions of degrees found in these extended vulnerable components (b), (e), and (h).

5(c)] than in the assortative networks [Fig. 5(i)]. In uncorrelated networks, vulnerable and stable vertices are likely to connect to one another [Fig. 5(d)], frustrating the formation of a sizable extended vulnerable component [Fig. 5(e)], hence prohibiting global cascades (Fig. 4).

As illustrated in Fig. 5, the probability with which a vertex of degree k is attached to the vulnerable component (and consequently, the frequency with which it triggers a global cascade) is highly influenced by degree-degree correlations. For an average degree z sufficiently above the percolation threshold, global cascades typically topple the entire network [8] (Fig. 3). Taken together, these two observations imply that the relationship between the degree of the vertex in which the initial seed is placed and the average size of the cascade (S_{avg}) it triggers is also heavily influenced by degree-degree correlations. To further illustrate this effect, we present in Fig. 6 the average cascade size for $\phi=0.18$ as a function of average degree z for varying assortativities [Figs. 6(a)–6(e)]. As in [13], we make the arbitrary distinction between high-degree vertices (those in the top 10% of the degree distribution p_k) and average degree z vertices (for networks with noninteger average degree z, the influence of an average degree vertex was calculated via linear interpolation between S_{avg} observed at $\lfloor z \rfloor$ and $\lceil z \rceil$, consistent with [13]). Here, we also report on cascades triggered by low-degree vertices (those in the bottom 10% of the degree distribution p_k).

As shown in Fig. 6, the relative influence of high-degree vertices is nonmonotonic, with maximum effect in uncorrelated networks and reduced effect at both negative and positive assortativities, while the relative influence of low-degree vertices increases monotonically as assortativity increases. As noted in [13], the average size of cascades triggered by high-degree vertices is marginally greater than those triggered by average degree vertices in uncorrelated networks, a result reproduced here in Fig. 6(c). This relationship holds for moderately disassortative networks [$r=-0.5$, Fig. 6(b)], but as networks become strongly disassortative [$r=-0.9$, Fig.

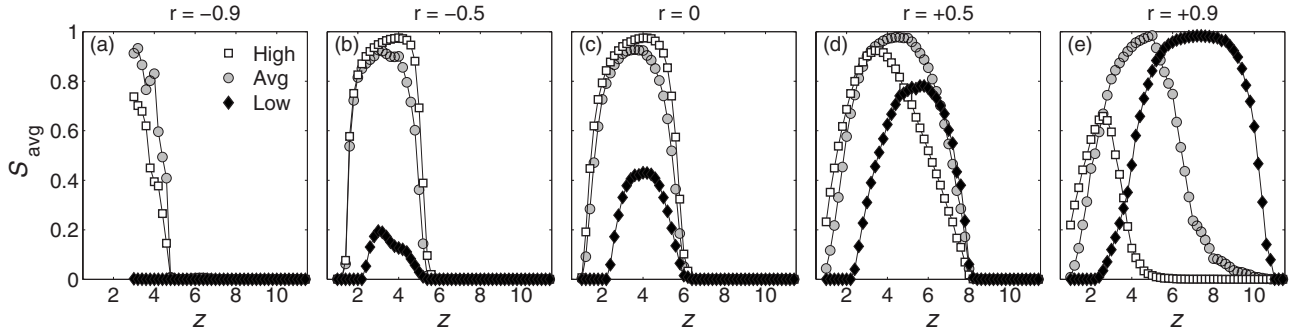

FIG. 6. Average cascade size with $\phi=0.18$ as a function of average degree z given that the initial seed was placed in high-degree vertices (in the top 10% of the degree distribution, squares), average degree vertices (circles), or low-degree vertices (in the bottom 10% of the degree distribution, diamonds), for random networks with (a) $r=-0.9$, (b) $r=-0.5$, (c) $r=0$, (d) $r=+0.5$, and (e) $r=+0.9$. Note that in (a), we were not able to obtain data for $z<3$ (Table I). Lines are provided as a guide for the eyes.

6(a)], the average size of cascades triggered by high-degree vertices falls below those triggered by average degree vertices. This occurs because the extreme disassortativity forces many high-degree vertices to connect to $k=1$ vertices, excluding them from Ω_v. In contrast, in strongly disassortative networks with very low z, average degree vertices often connect to one another and thus are frequently included in Ω_v. In networks with even moderately positive assortativity [Fig. 6(d)], the average cascade size triggered by average degree vertices exceeds those triggered by high-degree vertices, except in the sparsest (low z) networks, and this reversal becomes highly pronounced for dense networks (high z) and strong positive assortativity [$r=+0.9$, Fig. 6(e)]. In general, the size of cascades triggered by low-degree vertices increases as assortativity is tuned from strongly negative [Fig. 6(a)] to strongly positive [Fig. 6(e)]. In disassortative networks, low-degree vertices connect to high-degree stable vertices and thus cannot trigger cascades. On the other hand, for dense networks (high z) with strongly positive assortativity ($r=+0.9$), sizable information cascades are only triggered by low-degree vertices [Fig. 6(e)]. This occurs because highly connected stable vertices are likely to connect only with one another, forming stable clusters in Ω_x, whereas low-degree vulnerable vertices possess fewer connections and most often connect with one another, forming a dense core of vulnerable vertices in Ω_v, from which large cascades easily arise. Figure 6 also clarifies which vertices contribute to the expansion of the upper z boundary of the cascade window as assortativity increases (Fig. 1), with the emphasis shifting increasingly to lower degree vertices.

VI. DISCUSSION

In certain random networks of sufficient density (high average degree z), information cascades occur relatively infrequently, but when they do occur they often spread throughout the entire network [8]. Such systems have been characterized as "robust yet fragile" [20]. We have shown that increasing assortativity in a random network can exacerbate this effect, especially in networks whose degree-degree correlation is positive [Figs. 1 and 3(a)–3(d)]. Thus, not only do cascades occur more frequently in assortative networks but they also typically cover a greater proportion of the network. While this may be perceived as a blessing to marketing strategists, it is cause for concern regarding other forms of social contagion such as misinformation and disease. Conversely, the disassortative degree-degree correlations of technological and biological networks [1] may render these systems more resilient to small perturbations.

Increasing assortativity leads to an earlier onset (i.e., at lower z) of a percolating extended vulnerable component and an overall change in the shape of the functional relationship between global cascade frequency and average degree (Fig. 2). This result is in line with observations concerning the giant connected component in networks with heavy-tailed degree distributions [1]. However, in those networks, the maximum size of the giant connected component was found to be larger in disassortative networks than in uncorrelated or assortative networks [1]. Our experiments on random networks with Poisson degree distributions demonstrate that the size of the extended vulnerable component is largest when degree-degree correlations are assortative (Fig. 2).

In uncorrelated random networks with Poisson degree distributions, it is known [8] that global cascades starting from a single initial seed do not occur when $\phi>0.25$ [Fig. 1(b)]. However, for low average degree z, we observed global cascades for $\phi=0.33$ in both disassortative [Fig. 1(a)] and assortative [Fig. 1(c)] networks. This results in a bimodal response of cascade frequency to r and relatively smaller cascade sizes [Figs. 3(e) and 4], as compared to the unimodal response observed with $\phi\leq 0.25$ [Figs. 3(a) and 3(c)]. It is important to point out that bimodality only occurs for low average degree, which is a special case for disassortative networks.

Identifying which vertices will trigger large information cascades has long been of interest, both in applications where the desire is to promote such cascades (as in marketing [16]) as well as in applications where the desire is to prevent such cascades (as on the electrical power grid [10] or in epidemiology [6]). A common assumption among the social scientists and marketing strategists is that the most connected individuals (so-called "influentials") are the best candidates for triggering a sizable information cascade [16]. Recent results in uncorrelated random networks [13] have demonstrated that cascades resulting from seeding high-

degree vertices (those in the top 10% of the degree distribution) were actually not much larger than those emanating from vertices of average degree [this result is recreated in Fig. 6(c)]. Here, we found that cascades are possible in much denser networks that are positively assortative, and, in these networks, the low and average degree vertices are responsible for triggering the largest cascades [Figs. 6(d) and 6(e)], resulting from an amalgamation of vulnerable vertices (a similar result was obtained in [13] for group-based networks). This result may be of direct relevance to the social science and marketing communities and may speak to the relative success of viral marketing campaigns that leverage online social networking [21] such as the Obama campaign [22,23]. In contrast, in disassortative networks the cascade window is restricted to sparser networks and, in these networks, we found that cascades resulting from seeding high-degree and average vertices does result in much larger cascades [Figs. 6(a) and 6(b)] than those observed from seeds placed in low-degree vertices. These results may indicate that targeted infection of highly connected vertices may be an effective strategy for disseminating information in networks with negative degree-degree correlations, such as the Internet. Finally, we note that the phenomena reported here in both global cascade frequency and size are not apparent from the analytical treatments of this model [17,18], or from other models of information spreading on degree-correlated networks (e.g., [6]).

ACKNOWLEDGMENTS

The computational resources provided by the Vermont Advanced Computing Center which is supported by NASA (Grant No. NNX 08A096G) are gratefully acknowledged. J.L.P. and M.J.E were partially supported by Vermont EPSCoR (NSF Grant No. EPS 0701410).

[1] M. E. J. Newman, Phys. Rev. Lett. **89**, 208701 (2002).
[2] M. E. J. Newman, Phys. Rev. E **67**, 026126 (2003).
[3] A. Barrat, M. Barthélemy, and A. Vespignani, *Dynamical Processes on Complex Networks* (Cambridge University Press, New York, 2008).
[4] Y. Yin, D. Zhang, G. Pan, M. He, and J. Tan, Phys. Scr. **76**, 606 (2007).
[5] Z. Rong, X. Li, and X. Wang, Phys. Rev. E **76**, 027101 (2007).
[6] I. Z. Kiss, D. M. Green, and R. R. Kao, J. R. Soc., Interface **5**, 791 (2008).
[7] J. L. Payne and M. J. Eppstein, IEEE Trans. Evol. Comput. **13**, 895 (2009).
[8] D. J. Watts, Proc. Natl. Acad. Sci. U.S.A. **99**, 5766 (2002).
[9] M. L. Sachtjen, B. A. Carreras, and V. E. Lynch, Phys. Rev. E **61**, 4877 (2000).
[10] R. Kinney, P. Crucitti, R. Albert, and V. Latora, Eur. Phys. J. B **46**, 101 (2005).
[11] T. C. Schelling, J. Conflict Resolut. **17**, 381 (1973).
[12] J. P. Gleeson and D. J. Cahalane, Phys. Rev. E **75**, 056103 (2007).
[13] D. J. Watts and P. S. Dodds, J. Consum. Res. **34**, 441 (2007).
[14] D. Centola, V. M. Eguíluz, and M. W. Macy, Physica A **374**, 449 (2007).
[15] A. Galstyan and P. Cohen, Phys. Rev. E **75**, 036109 (2007).
[16] E. Katz and P. F. Lazarsfeld, *Personal Influence: The Part Played by People in the Flow of Mass Communications* (Free Press, Glencoe, IL, 1955).
[17] P. Dodds and J. Payne, Phys. Rev. E **79**, 066115 (2009).
[18] J. P. Gleeson, Phys. Rev. E **77**, 046117 (2008).
[19] This cascade condition bears some resemblance to Eq. (33) provided by Gleeson [18]. To connect them analytically, we translate Gleeson's expression into our notation. Gleeson finds that global cascades arising from an infinitesimally small seed fraction is possible if the largest eigenvalue of the following matrix exceeds unity: $B_{jk}=\frac{k-1}{q_{k-1}}b_k e_{j-1,k-1}$. By shifting indices, our condition can be modified as $0=\det[A_{jk}]=(\Pi_{k=1}^{\infty}q_{k-1})\det[\delta_{jk}-\frac{k-1}{q_{k-1}}b_k e_{j-1,k-1}]=(\Pi_{k=1}^{\infty}q_{k-1})\det[\delta_{jk}-B_{jk}]$, where we have replaced $\delta_{j-1,k-1}$ and δ_{jk}. This holds since multiplication by q_{k-1} affects the kth column uniformly and by multilinearity of determinants can be factored out. We now see that the conditions match in that when the matrix $[B_{jk}]$ has an eigenvalue equal to 1, the determinant of $[\delta_{jk}-B_{jk}]$ must be 0.
[20] J. M. Carlson and J. Doyle, Phys. Rev. Lett. **84**, 2529 (2000).
[21] B. Freeman and S. Chapman, J. Epidemiol. Community Health **62**, 778 (2008).
[22] B. Stelter, *The Facebooker Who Friended Obama* (The New York Times, New York, 2008).
[23] K. Tumulty, *Obama's Viral Marketing Campaign* (Time Magazine, New York, 2007).